



HAL
open science

Transient behavior and relaxations of the L3 (sponge) phase : T-jumb experiments

G. Waton, G. Porte

► **To cite this version:**

G. Waton, G. Porte. Transient behavior and relaxations of the L3 (sponge) phase : T-jumb experiments. *Journal de Physique II*, 1993, 3 (4), pp.515-530. 10.1051/jp2:1993148 . jpa-00247851

HAL Id: jpa-00247851

<https://hal.science/jpa-00247851>

Submitted on 4 Feb 2008

HAL is a multi-disciplinary open access archive for the deposit and dissemination of scientific research documents, whether they are published or not. The documents may come from teaching and research institutions in France or abroad, or from public or private research centers.

L'archive ouverte pluridisciplinaire **HAL**, est destinée au dépôt et à la diffusion de documents scientifiques de niveau recherche, publiés ou non, émanant des établissements d'enseignement et de recherche français ou étrangers, des laboratoires publics ou privés.

Classification

Physics Abstracts

42.20J — 82.70D — 66.10C — 61.25

Transient behavior and relaxations of the L_3 (sponge) phase : T-jump experiments

G. Waton ⁽¹⁾ and G. Porte ⁽²⁾

⁽¹⁾ Laboratoire d'Ultrasons et de Dynamique des Fluides Complexes (*), Université Louis Pasteur, 4 rue Blaise Pascal, 67070 Strasbourg Cedex, France

⁽²⁾ Groupe de Dynamique des Phases Condensées (*), Université Montpellier II, Case 026, Place Eugène Bataillon, 34095 Montpellier Cedex 05, France

(Received 26 October 1992, accepted 29 December 1992)

Abstract. — We report here on a systematic time resolved investigation of the transient behavior of the sponge phase after an abrupt temperature jump. We obtain evidence for three distinct relaxation times τ_1 , τ_2 and τ_3 having very different magnitudes. We show that τ_1 is related to a conserved internal variable while τ_2 and τ_3 both correspond to the relaxations of unconserved thermodynamic variables. We propose an interpretation of the transient behavior based on the idea that the temperature jump essentially puts the membrane in L_3 under transient tension. According to this interpretation, τ_1 corresponds to the relaxation of concentration fluctuations, τ_2 to that of the degree of symmetry of the structure and τ_3 to that of its density of connectivity. This picture actually accounts at least qualitatively for the experimental observation. Moreover, the temperature dependences of τ_2 and τ_3 close to the sponge-to-lamellar transition temperature indicate that this transition is quite weakly first order.

Introduction.

The anomalous isotropic phase L_3 in an amphiphilic system (sponge phase) provides an ideal experimental realization of an infinite fluid membrane multiconnected along the three directions of space with no long-range order [1-4]. Equilibrium properties such as the phase stability and the static structure factor and some dynamical properties close to equilibrium have been extensively studied and are in the course of being well understood. In comparison, understanding non-equilibrium properties is in a rather primitive stage [5, 6]. The present article aims at providing further experimental insights into this problem. More precisely, here we use the T-jump technique in order to evidence and measure the characteristic relaxation times that can be relevant for the dynamical properties of the L_3 phase.

(*) Associé CNRS.

The idea of a T-jump experiment is to put the given structure abruptly out of equilibrium by a sudden increase of its temperature and to follow how it goes to its new equilibrium state at this new temperature. In the present case, the sudden change in temperature is achieved by discharging a capacitor through the conducting brine swollen L_3 sample. And the relaxation of the structure is observed using time resolved measurements of the intensity scattered by the sample. This procedure is here appropriate since L_3 phases are known to scatter light very strongly specially at high dilutions.

Structures in complex fluid often exhibit several degrees of freedom at large scale, each of them having a characteristic relaxation time. In the favorable cases, these times are sufficiently different in magnitude and each degree of freedom will relax after the shortest ones are completely annealed and while the longest ones are still quenched. The different contributions can thus be resolved separately.

In section 1 we sum up some backgrounds : we recall the internal variables that define the thermodynamic state of sponge phases and the scaling behavior of their characteristic relaxation times. The experimental facts are reported in section 2. In section 3, we propose an interpretation of the transient oscillation of $I(q)$ in terms of the excess surface tension transiently imposed to the membrane by the ΔT step. The relevance of this interpretation is further discussed in section 4.

1. Background.

According to the structure commonly admitted for L_3 , it is convenient to consider the schematic drawing in figure 1. The basic features are the following. Most of the amphiphile self assembles into a bilayer defining an infinite surface free of rims and seams. The surface is isotropically multiconnected to itself in the three directions of space. And it divides space in two and only two distinct subvolumes v_1 and v_2 . Accordingly and following the analysis of Milner *et al.* in [7], we assume that the thermodynamical state of the phase at a given time is characterized by the average values of three internal variables :

- i) the area density of membrane a per unit volume (proportional to the volume fraction of amphiphiles ϕ),
- ii) the connectivity density n per unit volume (density of « handles » or « passages » in Fig. 1),
- iii) the degree of asymmetry Ψ between subvolumes v_1 and v_2 .

$$\Psi = \frac{v_1}{v_1 + v_2} - \frac{1}{2}. \quad (1)$$

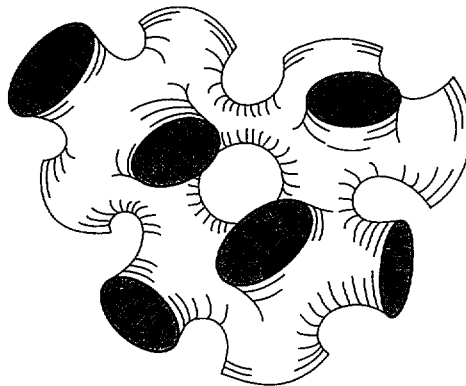


Fig. 1. — Schematic structure of the L_3 phase.

At equilibrium, \bar{a} and \bar{n} are related by a non-linear conservation relation $\bar{n} \sim \bar{a}^3$ expressing the scale invariance of the structure [4, 5] (the geometrical prefactor is determined by the equilibrium structure). Since the bilayer is locally symmetrical with respect to its mid surface, in general we expect $\bar{\Psi} = 0$. (Here we do not consider the very dilute cases where the so-called inside/outside symmetry [8] is spontaneously broken, at equilibrium, at global scale.)

Out of equilibrium, the conservation relation and the symmetry can be however transiently broken at global scale. Note that while a is indeed a conserved variable (concentration of amphiphiles), n and Ψ are not. Accordingly, we expect two relevant characteristic times. The first one, τ_n , is the relaxation time of the connectivity. It is indeed related to the average life time τ_h of one given « passage ». According to [7] it has the form :

$$\tau_h = \tau_0 \exp\left(\frac{E_A}{k_B T}\right) \quad (2)$$

where τ_0^{-1} is the average frequency of membrane collisions in the passage and E_A is the activation energy involved in one elementary change in the membrane topology. Then, it is straightforward to show that τ_n has the form :

$$\tau_n = \tau_h \left[\frac{k_B T}{\bar{n} (\partial^2 f / \partial n^2)} \right] \quad (3)$$

where f is the free energy density of the L_3 phase at equilibrium. Simple scaling arguments discussed at length in [5] then imply that τ_n scales like $\phi^{-3}(\bar{a}^{-3})$.

The second time, τ_Ψ , is the relaxation time of the symmetry. It is controlled by the transport of the solvent from subvolume 1 to subvolume 2 through the membrane. The hydrophobic core of the bilayer being presumably quite impermeable to the brine solvent, we expect τ_Ψ to be rather related to the average equilibrium density of « pores » in the membrane [7]. Whatever the actual transport mechanism, we can assume a permeability parameter π_t per unit area of bilayer. So that :

$$dv_1/dt = -\Delta p \cdot \pi_t \cdot a \quad (4)$$

where Δp is the pressure difference between subvolumes 1 and 2. At equilibrium ($\bar{\Psi} = 0$) $\Delta p = 0$, but more generally :

$$\Delta p = -\Psi \frac{\partial^2 f}{\partial \Psi^2} \quad (5)$$

We obtain :

$$\tau_\Psi = \pi_t \cdot \frac{\partial^2 f}{\partial \Psi^2} \cdot \bar{a} \quad (6)$$

Remembering that $\bar{a} \sim \phi$ and $\partial^2 f / \partial \Psi^2 \sim \phi^3$ (from the usual scaling argument [5]), we immediately see that τ_Ψ scales like ϕ^{-4} along a dilution line (constant π_t).

These relaxation times are here specially important : they define the time scales below which \bar{n} and $\bar{\Psi}$ are quenched (and therefore must be considered as conserved variables) and beyond which they are annealed (unconserved). Attempting to predict their relative magnitudes would be rather speculative since they are presumably strongly system dependent (due to the permeability factor π_t).

2. Experimental facts.

The experimental set up has been described in detail in [9]. The amplitude ΔT of the T step imposed to the sample (typically a few tenths of a °C) is adjusted by monitoring the charge tension of the capacitor. A xenon-mercury lamp is used to illuminate the sample. Incident monochromatic wavelengths are selected using interferential filters : $\lambda = 577$ nm and 405 nm. The scattered intensity is collected at two different angles off the incident beam. Combining wavelengths and angles, four values of q 's are available ($q = 0.50 \times 10^5 \text{ cm}^{-1}$, $q = 0.72 \times 10^5 \text{ cm}^{-1}$, $q = 2.05 \times 10^5 \text{ cm}^{-1}$, $q = 2.92 \times 10^5 \text{ cm}^{-1}$) so that the q dependence of the relaxation times can be estimated.

The system investigated is the system CPCl/hexanol/brine (0.2 M NaCl) for which we have previously collected the most complete set of structural data [1]. We studied three samples in the L_3 monophasic domain. Their composition in CPCl and hexanol (Tab. I) are chosen so that they roughly correspond to the same dilution line. Comparing the data obtained on these samples, we can estimate the dependence of the relaxation times as a function of the volume fraction ϕ of membranes ($\phi = 0.026$, $\phi = 0.053$, $\phi = 0.072$). Actually we could not investigate more concentrated samples for which the response is too low and therefore the signal-to-noise ratio does not allow an appropriate resolution.

Table I. — *Composition of the investigated samples. $T_{L_3 \rightarrow L_\alpha}$ is the temperature of the L_3 to L_α transition.*

CPCl (g/100g)	n-hexanol (g/100g)	ϕ	$T_{L_3 \rightarrow L_\alpha}$
1.09	1.41	0.026	15°C
2.28	2.72	0.053	8°C
3.11	3.57	0.072	1°C

In contrast with other systems [10], the L_3 phase in the present system *does not show* the characteristic critical behavior related to the spontaneous Ψ symmetry breaking at high dilutions. Upon increasing dilution beyond $\phi = 0.011$, the L_3 phase here rather stops swelling and simply phase separates expelling excess brine. So, at equilibrium, the L_3 phase of the present system has the structure of a symmetric sponge ($\Psi = 0$) all over its domain of stability. On the other hand, the L_3 structure of the three samples investigated has a limited temperature range of stability : more precisely, all three samples eventually phase separate with the L_α phase (swollen lamellar phase) upon decreasing temperature. The transition temperatures respectively measured for each sample are given in table I. We performed T-jump measurements at different temperatures, and so we could evidence interesting slowing down of two relaxation processes when approaching the L_3 to L_α transition temperature.

Usually, in a T-jump experiment, the scattered intensity varies monotonically from its initial to its final equilibrium values, thus reflecting the monotonic evolution of the system towards

its final state. In the present case of sponge phase samples, the behavior is very different : a typical response is represented in figure 2. First we note, that the initial and final values of the scattered intensity are very close to each other. This is actually consistent with static light scattering data which have shown that the intensity scattered by sponge phases at equilibrium is quite insensitive to temperature : typically a few percent variation or so *per* °C. But what is especially impressive here, is the very large oscillation of $I(q)$ observed transiently in between the two almost identical initial and final values. The amplitude of the oscillation reaches in the most favorable cases (most dilute sample with $\Delta T \sim 0.5$ °C) about 30 % of the equilibrium values. The amplitude of the effect appears to be roughly linear with the amount of energy injected by the electric discharge into the sample (i.e. linear with ΔT) as shown for an example in figure 3. Owing to this *non monotonic* variation having a large enough amplitude, the transient behavior of the sponge phase can be investigated with a reasonable accuracy.

We clearly observe three distinct time ranges in figure 2b with which we associate the respective characteristic times τ_1 , τ_2 and τ_3 . We performed many measurements varying the experimental conditions in order to determine the variation of the transient behavior *versus* the variations of the three experimental parameters : q , ϕ and T . For all sets of experimental parameters, the general transient pattern remains similar in shape to that of figure 2b : only the magnitude of the amplitude and of the relaxation times τ_1 , τ_2 and τ_3 changes from one set to the other. We sum up below the results of this systematic investigation.

During step 1, the intensity first increases quickly. For the most concentrated sample $\phi = 0.072$ at high q ($q = 2.05 \times 10^5 \text{ cm}^{-1}$ and $q = 2.92 \times 10^5 \text{ cm}^{-1}$) this step is too fast to be analyzed within the time resolution of the experimental set up. The situation is better with the other two samples. Actually, the $I(q)$ increase is not well fitted with a single exponential, and a more detailed analysis is made uneasy due to the onset of the following step 2 where the $I(q)$ variation changes sign. In spite of this difficulty, the order of magnitude of τ_1 can be estimated. As shown in the example given in table II, it appears to be proportional to

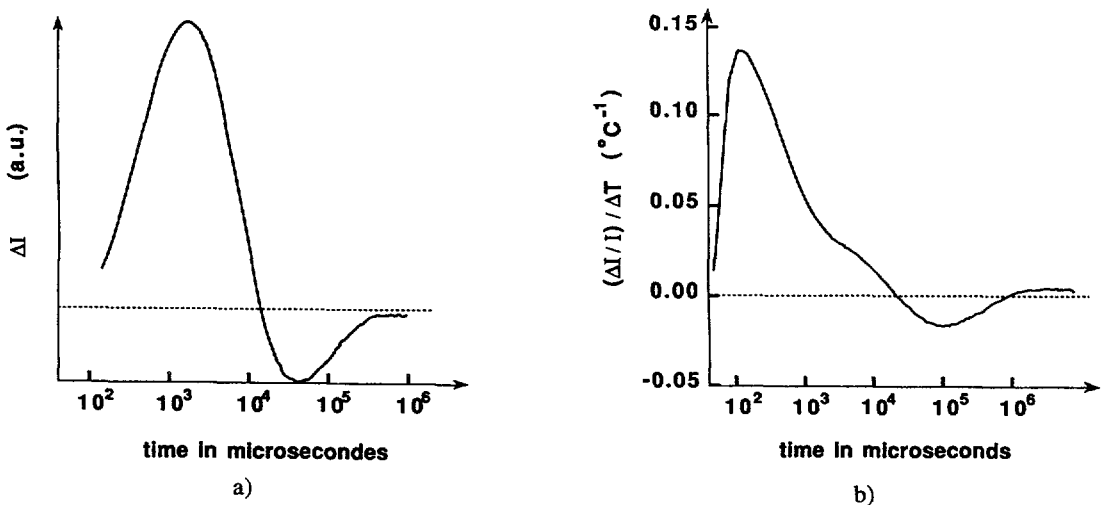


Fig. 2. — a) Evolution of the turbidity (intensity over all q 's) as a function of time after the ΔT step. The horizontal straight line corresponds to the initial value. Sample $\phi = 0.053$, $T = 35$ °C, $\Delta T = 0.5$ °C. b) Evolution of the intensity scattered at $q = 2.92 \times 10^5 \text{ cm}^{-1}$ as a function of time after the ΔT step. Same sample and experimental conditions as in figure 2a but $T = 19$ °C.

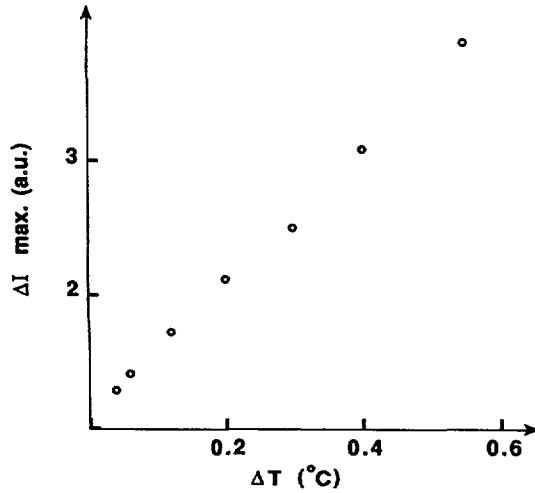


Fig. 3. — Amplitude of the oscillation of $I(q)$ as a function of the ΔT step. Sample $\phi = 0.053$, $T = 19^\circ\text{C}$, $q = 2.92 \times 10^5 \text{ cm}^{-1}$. The effect is roughly linear versus ΔT .

Table II. — τ_1 , τ_2 and τ_3 at different q^2 's. Sample $\phi = 0.053$, $T = 17^\circ\text{C}$.

q^2 (10^{+10} cm^{-2})	τ_1 (ms)	τ_2 (ms)	τ_3 (ms)
0.51	2.5	24	490
0.25	4.9	27	460

q^{-2} Moreover, when τ_1 can be estimated with enough accuracy (dilute samples and low q 's), it happens to be quite close to the characteristic time measured by quasi-elastic light scattering under the same conditions (proportional to ϕ^{-1} and q^{-2}). Therefore it is reasonable to associate step 1 with a diffusion process having basically the same dynamics as the spontaneous concentration fluctuations in the sample. On the other hand, τ_1 shows no appreciable temperature dependence with no particular slowing down when T approaches the L_3 to L_α transition temperature.

During the second step (step 2), the scattered intensity decreases down to a second intermediate value. For the two most dilute samples ($\phi = 0.026$, $\phi = 0.053$), the first two steps have characteristic times sufficiently different in magnitude making so the analysis reliable. At the beginning of step 2, the scattered intensity starts decaying in a non-single exponential way and within times that are q -dependent. After a while, however, the $I(q)$ decay becomes *single exponential and q -independent* (see Tab. II for an example). This characteristic time, which we hereafter denote τ_2 , decreases very fast upon increasing concentrations. In order to illustrate this steep ϕ dependence, we have plotted in figure 4 the evolutions of τ_2 versus temperature for the two most dilute samples. Actually, these evolutions

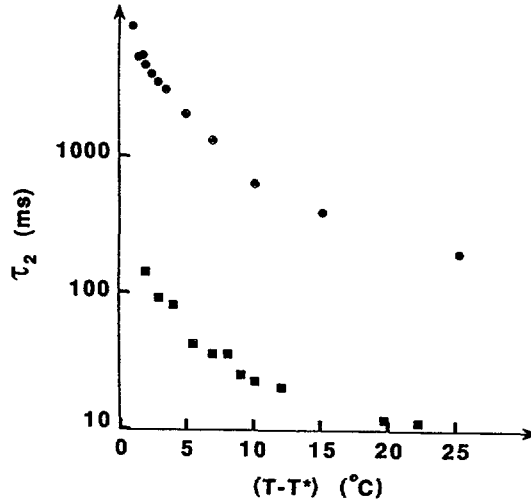


Fig. 4. — The relaxation time τ_2 versus $(T - T^*)$ for the two dilute samples. Full circles $\phi = 0.026$, full squares $\phi = 0.053$. T^* is the temperature where τ_2 diverges : T^* is very close to the L_3 to L_α transition temperature.

are quite parallel to one another when plotted versus the difference $(T - T^*)$ between the actual temperature T and a reference temperature T^* close to the L_3 to L_α transition temperature. The τ_2 s for these samples are found in the ratio 1/40 while their volume fractions are in the ratio 1/2. This means a ϕ dependence for τ_2 even steeper than the ϕ^{-4} power law expected for τ_ψ in the preceding section.

Due to this very steep ϕ dependence, τ_2 for the most concentrated sample ($\phi = 0.072$) becomes of the same order of magnitude as τ_1 (which shows a much softer ϕ dependence $\sim \phi^{-1}$), and a separate quantitative analysis of step 1 and step 2 can no longer be performed on safe grounds for that sample.

On the other hand, the temperature dependence of τ_2 (for the other two samples) is also very strong (Figs. 4 and 5). We have checked that it does *not* correspond to a simple Arrhenius behavior. Actually, it rather suggests some kind of a «critical slowing down» when approaching the L_3 to L_α phase transition. This point of view is further supported when plotting $(\tau_2)^{-1}$ versus T as shown in figure 5b. Actually, the points corresponding to temperatures not too far from the transition temperature are well aligned along a straight line : extrapolating this straight line down to $(\tau_2)^{-1} = 0$ yields a «critical» temperature T^* which happens to be quite close to the transition temperature (within 1 °C at most). This fact is surprising since we know that a thin but well defined two-phase region separates L_α from L_3 in the phase diagram : the L_3 to L_α transition is therefore certainly first order. If the present interpretation in terms of «critical slowing down» is correct, the fact that T^* is so close to the transition temperature implies that the first order character of the L_3 to L_α transition is quite weak.

During the third step, the scattered intensity increases again and finally reaches its new equilibrium value corresponding to the temperature $T + \Delta T$. For all three samples, τ_3 is found to be very large compared to τ_2 and a quantitative analysis is in principle reliable. For the most dilute sample ($\phi = 0.026$) however, τ_3 is actually so long (> 10 s even at high temperatures) that it stands beyond the upper limit in time range resolved by the experimental set up. For the other two samples ($\phi = 0.053$ and $\phi = 0.072$) τ_3 has a more appropriate order

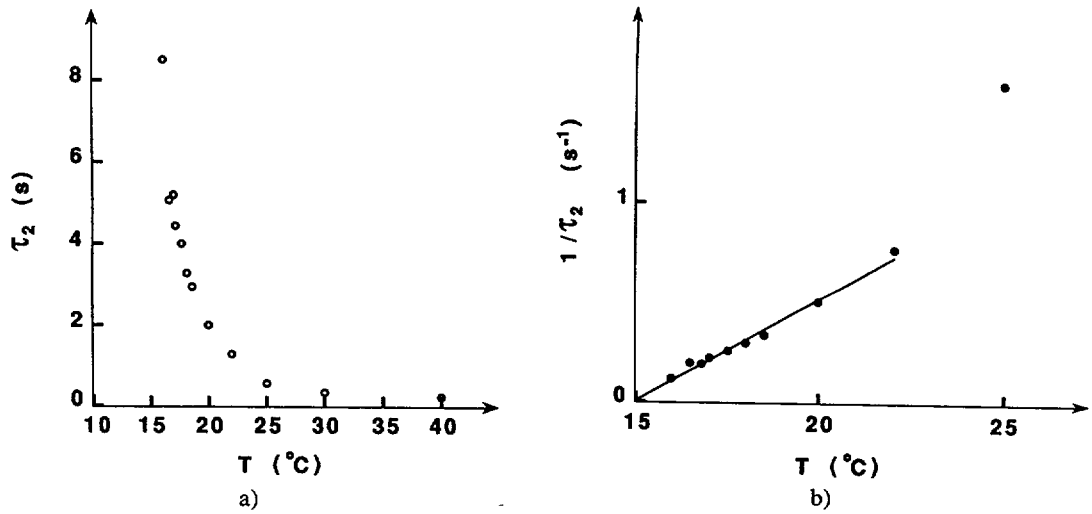


Fig. 5. — a) The relaxation time τ_2 versus T . Sample $\phi = 0.026$. b) The inverse relaxation time $(\tau_2)^{-1}$ versus T ; same sample. This plot defines the « critical » temperature T^* which happens to be very close to the L_3 to L_α transition temperature (see Tab. I).

of magnitude. The relaxation is actually very well fitted with a *single exponential* and it is found remarkably *independent of the wave vector* (see Tab. II for an example). Comparing the temperature variations of τ_3 for the two samples (Fig. 6), one sees that it strongly depends on the concentration ϕ . More quantitatively, this comparison suggests that τ_3 scales as ϕ^{-3} as expected for the relaxation time τ_n of the topology (see (3) in the preceding section). On the other hand, τ_3 also shows a strong temperature dependence (Figs. 6 and 7) which is not of the Arrhenius type but again suggests some critical slowing down related to the $L_3 \rightarrow L_\alpha$

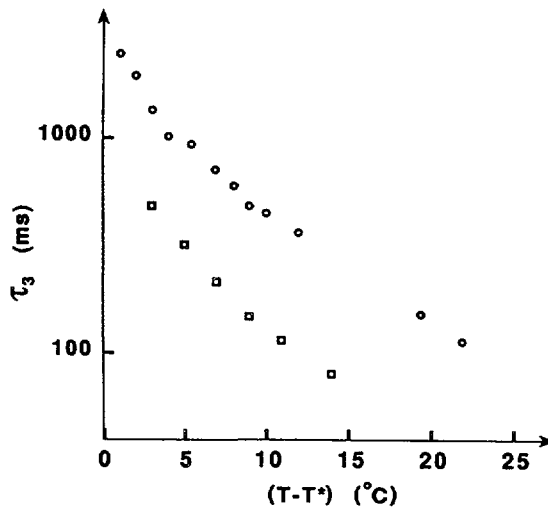


Fig. 6. — The relaxation time τ_3 versus $(T - T^*)$ for the two more concentrated samples. Circles $\phi = 0.053$, squares $\phi = 0.072$. T^* is the temperature where τ_3 diverges: T^* is very close to the L_3 to L_α transition temperature.

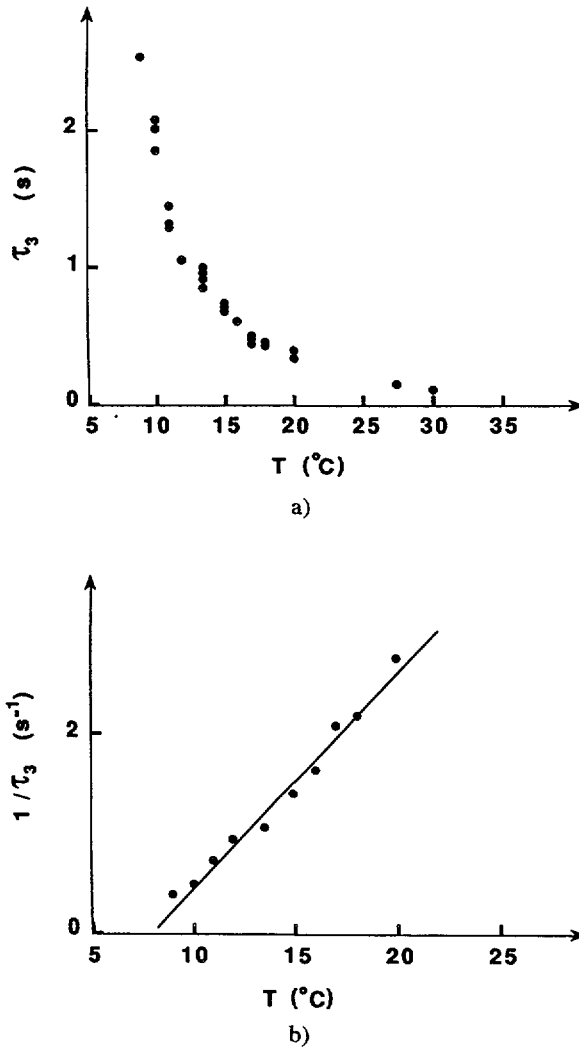


Fig. 7. — a) The relaxation time τ_3 versus T . Sample $\phi = 0.053$. b) The inverse relaxation time $(\tau_3)^{-1}$ versus T ; same sample. This plot defines the « critical » temperature T^* .

transition. Actually, using for τ_3 the same plot as we did for τ_2 (Fig. 7b), one obtains the same type of straight evolution which defines a characteristic temperature $T_{\tau_3}^*$. Here again, $T_{\tau_3}^*$ is found quite close to the actual transition temperature. Moreover, the fact that τ_2 and τ_3 have very different magnitudes allows a quantitative treatment accurate enough for a reliable estimation of the amplitude A_3 related to τ_3 . In figure 8 the variations of A_3 versus T for the intermediate sample are shown: clearly A_3 decreases upon decreasing temperature and extrapolates to zero close to the $L_3 \rightarrow L_\alpha$ transition temperature.

As a final remark for this section, the ϕ dependences of τ_2 and τ_3 are indeed important for the analysis in terms of scaling behavior. Unfortunately, we could not check them with enough accuracy. For the most concentrated sample, τ_2 is quite mixed up with τ_1 , while for the most dilute sample τ_3 is too long for a quantitative analysis. So the ϕ dependences are checked on two samples respectively. If we believe the indications obtained on two samples only,

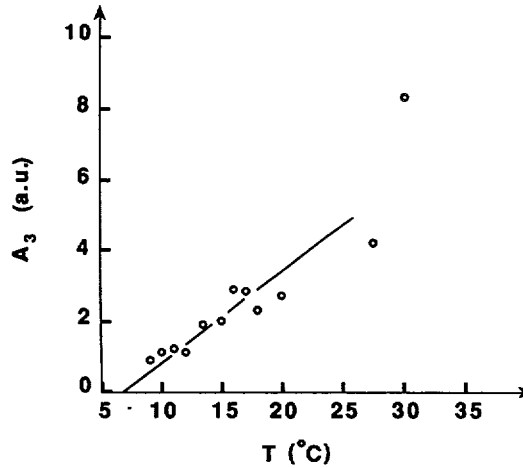


Fig. 8. — Amplitude A_3 related to τ_3 as a function of T . Same sample as in figure 7 ($\phi = 0.053$). A_3 vanishes close to T^* .

τ_3 is found to scale as ϕ^{-3} . On the other hand, τ_2 is found to vary in a steeper way than ϕ^{-3} or even ϕ^{-4} . From this observation, we should conclude that τ_2 corresponds neither to $\tau_n(\phi^{-3})$ nor to $\tau_\psi(\phi^{-4})$. However, we must keep in mind that the scaling law for τ_ψ (6) is obtained assuming that the permeability of the membrane is the same in samples of different concentrations ϕ (identical density of pores). This condition is in principle satisfied along an exact dilution line where the chemical composition of the membrane in surfactant and cosurfactant is exactly constant. In the present system, the n-hexanol has an appreciable solubility in the brine solvent and we know of no means to be sure of what proportion is molecularly dissolved in the solvent and what is actually involved in building up the bilayer. Hence, there is very little chance for our three samples to belong to the same exact dilution line. Finally, the most we can say at the present time is that the steep ϕ dependences observed for τ_2 and τ_3 are qualitatively in favour of the idea that they correspond to τ_ψ and τ_n , respectively.

3. Interpretation.

The transient behavior of L_3 after the T -jump is very unusual. Instead of the classical monotonic variations of $I(q)$, we here observe a large amplitude oscillation in between almost identical initial and final values. In section 1, we mentioned that any thermodynamical state of L_3 can be defined by the average values of the three internal variables: a , n and Ψ . The first is a conserved variable while the other two are not. Interestingly, τ_1 is found to vary like q^{-2} while τ_2 and τ_3 are independent of the wave vector. τ_1 thus corresponds to a diffusion process and therefore is related to a conserved quantity. On the other hand, τ_2 and τ_3 are typical of the relaxation of unconserved quantities. It is therefore tempting to relate τ_1 to a and τ_2 and τ_3 to the other two variables i.e. Ψ and n (or conversely). This idea is further supported by the observation that τ_2 and τ_3 show steep dependences *versus* ϕ which seems consistent with the scaling expectation for $\tau_\psi(\phi^{-4})$ and $\tau_n(\phi^{-3})$. We must keep in mind however that $I(q)$ essentially measures the q -component of the concentration fluctuations in the sample. Therefore, the evolutions in time of the internal variables are here probed through their indirect effect on the osmotic compressibility of the sample.

The purpose of the electric discharge through the sample is indeed to generate a quick temperature variation in the mixture. Actually, the time constant of the capacitor plus the resistance of the cell are extremely short ($\ll 1 \mu\text{s}$) so that the sample is homogeneously driven to the new temperature $T + \Delta T$ much before any structural relaxation can occur. The effect of the temperature variation on the final values of the susceptibilities related to the three internal variables is presumably very mild since $I(q)$ is almost identical in the initial and final states. However, one of them at least is subjected to strong transient variations, and this is what we try to interpret hereafter.

We expect that the ΔT step has two very quick effects. First, it will slightly enhance, the amplitude of the thermal curvature fluctuations of the membranes of wave vectors larger than \bar{d}^{-1} where \bar{d} is the characteristic structural length (diameter of the average « passage » see Fig. 2). Due to the high q range involved, the rise time for such enhancement of the membrane roughness is certainly shorter than any large scale structural relaxation. The second effect is related to the chemical components of the membrane which both (but more especially hexanol) have finite solubilities in the brine solvent. The solubilities increase with the temperature and ΔT will thus lead to a dissolution of a small portion of the total area of membrane into the solvent. This effect takes place at the molecular level so that we expect again its characteristic time to be very small and unobservable. Both the enhancement of the membrane roughness and the partial dissolution have as a basic common consequence to put *the membrane under transient tension*.

Besides the simple ΔT step, other effects of the electric discharge might plausibly occur. It is known that, when submitted to moderate alternative electric fields, lipid bilayers oscillate accordingly. This reveals that the pressure of the free ions onto the membrane due to the electric field is capable of moving the bilayer. In the present experiment, where the transient electric field is of the order of a kV/cm or so, we could imagine that the multiconnected structure of L_3 might well explode completely due the transient excess local pressure. However, a similar transient destruction of the structure can be achieved by vigorous sonication. In this case, the mixture recovers its characteristic streaming birefringence after a few minutes which is much longer than the longest relaxation time observed in the T-jump experiment. So we believe that the structure of L_3 is not totally destroyed after the electric discharge. This guess is further supported by the fact that the response is roughly proportional to the electric energy dissipated in the sample (Fig. 3). The possibility remains however that small pieces of bilayers are torn off the infinite membrane by the pressure strike induced by the transient electric field. The small pieces would then immediately close up in the form of vesicles decorating the remaining infinite surface. Also, the holes reminiscent of the torn pieces would anneal within extremely short times (small holes). Then the return back to equilibrium requires that the small vesicles reintegrate into the infinite membrane. This implies local fusion of membranes and therefore would take quite a long time typically of the order of τ_h . So, here again, this mechanism leads to a transient reduction of the total area of bilayer available in the infinite membrane and therefore *put it under tension*.

We assume hereafter that this transient excess tension is the leading out of equilibrium thermodynamic parameter to be relaxed along the next steps and structural changes.

At the end of this initial very quick step (basically unobservable), the large scale structure of the infinite surface is just the same as before the ΔT step (same \bar{a}_{eff} , \bar{n} and $\bar{\Psi}$) but it is now under tension. Note that, here and below, a_{eff} represents the « effective » area density of surface : we mean here the area value that remains after having integrated or smoothed out the short wavelength thermal ripples of the surface (see Refs. [5, 11] for more details). Within this frame, although we expect a reduction of the *true* area of membrane (\bar{a}) just after the discharge, the *effective* area (\bar{a}_{eff}) remains unchanged as long as no large scale structural

changes have taken place. In this sense, the tension is related to the transient misfit between the « effective » and the « true » area densities.

Any mechanism allowing the average density of effective area \bar{a}_{eff} to decrease towards its new equilibrium value $\bar{a}_{\text{eff}}(T + \Delta T)$ ($< \bar{a}_{\text{eff}}(T)$) will release some of the excess tension. On time scales much shorter than τ_n and τ_Ψ , both \bar{n} and $\bar{\Psi}$ must be considered as frozen. But in spite of these constraints, there remains the possibility to partially release tension through enhancement of the low q 's ($q \ll \bar{d}^{-1}$) fluctuations of $\Psi(r)$. This possibility is quite clear when considering again the schematic drawing of figure 1. Starting from the symmetric picture and making a parallel displacement of the surface either towards the 1 or towards the 2 subvolume actually yields a symmetrical reduction of the effective area of the surface. Accordingly, we can express \bar{a}_{eff} in the form :

$$\bar{a}_{\text{eff}} = a^* (1 - \alpha_0 \bar{\Psi}^2) \quad (7)$$

where a^* represents the effective area density for a structure with the same connectivity density but with everywhere $\Psi(r) = 0$, and where α_0 is a geometrical factor of order unity. The absence of a term linear in Ψ simply expresses the intrinsic local symmetry of the membrane. In (7), it is obvious that an increase of the average square amplitude of the Ψ fluctuations (around $\bar{\Psi} = 0$) will reduce \bar{a}_{eff} and ultimately relax part of the excess tension. More generally, our statement is that the tension renormalizes (enhances) the susceptibility of Ψ and owing to the quadratic coupling between $\Psi(r)$ and the local concentration discussed at length in [8], the tension ultimately drives the variations of the scattered light intensity.

To make this picture more rigorous, it is convenient to build up a simple Landau Hamiltonian. The scale invariance of phases of fluid membranes discussed at length in [5] implies a very simple form for the free energy density of the phase :

$$f = \lambda a + B a^3 \quad (8)$$

where we neglect the logarithmic corrections [5, 8] which here have no dramatic consequences. λ is independent of the actual large scale structure of the phase, but, on the other hand, B depends on the internal variables n and Ψ . We therefore expand B in the form :

$$B = B_0 + B'' \left(\frac{n - \tilde{n}(a, \Psi)}{\tilde{n}(a, \Psi)} \right)^2 + B' \Psi^2 + D \Psi^4 \quad (9)$$

where $\tilde{n}(a, \Psi)$ represents the optimum value of n at fixed a and Ψ . Note that the couplings between n , a and Ψ are entirely specified by the definition of the optimum value $\tilde{n}(a, \Psi)$.

And therefore there is no term of order $\left(\frac{n - \tilde{n}(a, \Psi)}{\tilde{n}(a, \Psi)} \right) \Psi^2$. According to the scale invariance and to the symmetry in Ψ , $\tilde{n}(a, \Psi)$ takes the form :

$$\tilde{n}(a, \Psi) = \eta a^3 (1 + \alpha \Psi^2) \quad (10)$$

where η is a geometrical factor characterizing the equilibrium large scale structure, and $\alpha = 3 \alpha_0$. Combining (8), (9) and (10), we can specify the appropriate thermodynamic potential :

$$\Phi = f - \mu a \quad (11)$$

which is minimum for the equilibrium values of \bar{a} , \bar{n} and $\bar{\Psi} (= 0)$ (imposing the actual concentration \bar{a} of the sample determines μ). Let a_0 and $n_0 = \eta a_0^3$ be appropriate reference values :

$$a = a_0 \left(1 + \frac{\Delta a}{a_0} \right) \quad \text{and} \quad n = n_0 \left(1 + \frac{\Delta n}{n_0} \right). \quad (12)$$

Then Φ can be taken of the form :

$$\Phi = \Phi_0(a_0, n_0, 0) + \Delta\Phi \left(\frac{\Delta a}{a_0}, \frac{\Delta n}{n_0}, \Psi \right) \quad (13)$$

$\Delta\Phi$ is the appropriate Hamiltonian H . Specifying a_0 to be such that : $(\lambda - \mu) a_0 + B_0 a_0^3$ is minimum, one obtains after some manipulations :

$$\begin{aligned} \frac{H}{a_0^3} = \frac{\Delta\Phi}{a_0^3} = & 3 B_0 \left(\frac{\Delta a}{a} + \frac{B'}{2 B_0} \Psi^2 \right)^2 + B'' \left(\frac{\Delta n}{n} - 3 \frac{\Delta a}{a} - \alpha \Psi^2 \right)^2 + \\ & + B' \Psi^2 + \left(D - \frac{3 B'^2}{4 B_0} \right) \Psi^4 \quad (14) \end{aligned}$$

In (14), the equilibrium Hamiltonian is diagonalized and expressed in terms of three independent variables that are linear combinations of the initial variables a , n and Ψ . Far from critical conditions, we can neglect the influence of the Ψ^4 term and H is Gaussian. In this limit, it is in principle possible (although probably quite complicated due to the couplings between a , n and Ψ) to compute $\langle a(0) a(r) \rangle$ and so to derive the $I(q)$ pattern at equilibrium.

But our purpose is different : it is to understand the effect of the transient surface tension on the susceptibilities in (14). Just after the ΔT step, the « true » area density is forced towards a lower value while the connectivity density is still quenched at its initial value, this transient misfit being at the origin of the tension. Corresponding to these transient constraints on \bar{a} and \bar{n} , we introduce two Lagrange multipliers and define H_1 .

$$H_1 = H + \gamma(t) a + \nu(t) n \quad (15)$$

where $\gamma(t)$ represents the transient tension and $\nu(t)$ is the transient chemical potential of the connectivity which maintains \bar{n} at its initial value in spite of the tension. Then H_1 takes the form :

$$\begin{aligned} H_1 = & 3 B_0 a_0^3 \left(\frac{\Delta a}{a} + \frac{B'}{2 B_0} \Psi^2 \right)^2 + B'' a_0^3 \left(\frac{\Delta n}{n} - 3 \frac{\Delta a}{a} - \alpha \Psi^2 \right)^2 + \\ & + (\gamma(t) a_0 + 3 \nu(t) n_0) \left(\frac{\Delta a}{a} + \frac{B'}{2 B_0} \Psi^2 \right) + \nu(t) n_0 \left(\frac{\Delta n}{n} - 3 \frac{\Delta a}{a} - \alpha \Psi^2 \right) \\ & + B'_1 a_0^3 \Psi^2 + \left[D - \frac{3 B'^2}{4 B_0} \right] a_0^3 \Psi^4 \quad (16) \end{aligned}$$

where the inverse susceptibility $B'_1 a_0^3$ of Ψ is now shifted from its initial value $B' a_0^3$:

$$B'_1 a_0^3 = B' a_0^3 \left[1 - \frac{(\gamma(t) a_0 + 3 \nu(t) n_0)}{2 B_0 a_0^3} + \frac{\nu(t) n_0 \alpha}{B' a_0^3} \right]. \quad (17)$$

Considering (16) and (17), we see that, as expected from the former qualitative discussion, the transient tension here expressed by $\gamma(t)$ (and $\nu(t)$) essentially modifies the susceptibility of Ψ . Besides, the susceptibilities of the other two independent variables involving also n and a remain unaffected.

Minimizing H_1 versus $\Delta a/a$ and $\Delta n/n$ and imposing that the forced transient equilibrium values are $\frac{\Delta a}{a}(T + \Delta T)$ and $\frac{\Delta n}{n}(T + 0) = 0$ we eliminate $\gamma(t)$ and $\nu(t)$. Then B_1' takes the simple following form :

$$B_1' \equiv B' \left[1 + 2 \frac{B''}{B'} \alpha \left(3 \Delta \left(\frac{\Delta a}{a} \right)_{\Delta T} + \alpha (\Delta \overline{\Psi^2}(t)) \right) \right]$$

$$\text{with :} \quad \Delta \left(\frac{\Delta a}{a} \right)_{\Delta T} = \frac{\Delta a}{a}(T + \Delta T) - \frac{\Delta a}{a}(T + 0) \quad (18)$$

$$\text{and :} \quad \Delta \overline{\Psi^2}(t) = \overline{\Psi^2}(t) - \overline{\Psi^2}(0)$$

and with this convenient expression we are in a good position to analyse the time evolution of the scattered intensity.

Just after the T-jump ($t = 0$), the area of membrane is abruptly shifted down by an amount represented by $\Delta \left(\frac{\Delta a}{a} \right)_{\Delta T}$ (< 0). Since nothing else happens at the very beginning $\overline{\Psi^2}(t = 0)$ is still at its initial value so that $\overline{\Psi^2}(t = 0) = 0$. According to (18), the inverse susceptibility B_1' of Ψ is thus shifted down by an amount that can be large provided that B''/B' is much larger than 1. Therefore the thermal fluctuations of Ψ have the tendency to increase and correlatively (owing to the coupling) so does the scattered intensity. However, on short time scales ($\ll \tau_\Psi$) the membrane is impermeable to the solvent. Thus increasing $\langle \Psi_q \Psi_{-q} \rangle$ implies transport of solvent over distances of the order of q^{-1} . Correlatively, some amount of membrane area is also transported from places where Ψ^2 is higher towards places where it is lower. Therefore the corresponding increase in $I(q)$ essentially takes a time of the order of the diffusion time ($\sim q^{-2}$) that can be measured by classical quasi-elastic light scattering at the same wavevector. This is basically what we observe during the step τ_1 in figure 2.

Accordingly, we expect the higher q 's fluctuations of Ψ to increase faster than the lower q 's. So just after the ΔT -jump only the highest q 's fluctuations of Ψ are enhanced first. Afterwards, as time goes on, this excitation propagates progressively along lower q 's and correlatively $\overline{\Psi^2}(t)$ increases monotonically and therefore relaxes more and more the excess tension. This *feed back* effect actually appears in (18) where the monotonically increasing term $\Delta \overline{\Psi^2}(t)$ compensates more and more the initial effect of $\Delta \left(\frac{\Delta a}{a} \right)_{\Delta T}$ on the Ψ susceptibility as time goes on. Thus, after the time range τ_1 , $\Delta \overline{\Psi^2}(t)$ keeps increasing due to the excitation of Ψ modes of wave vectors smaller than that of the observation and B_1' increases accordingly (Eq. (18)). Then the intensity $I(q)$ scattered at the wave vector of observation starts decreasing at $t > \tau_1$. As long as $t < \tau_\Psi$, Ψ remains a conserved variable and the initial steps of the $I(q)$ decay (at $t > \tau_1$) remain q dependent and not single exponential. However, when t becomes larger than τ_Ψ , the permeability of the membrane becomes efficient and Ψ is no longer a conserved variable. Then all the very low q (such that $(Dq^2)^{-1} > \tau_\Psi$ where D is the diffusion coefficient) Ψ modes are excited together with the same characteristic time τ_Ψ which becomes therefore also the characteristic time of the partial tension relaxation. Accordingly, the tail of the $I(q)$ decay during the step τ_2 should be q independent and single

exponential. Again, these qualitative expectations on the $\dot{I}(q)$ decay actually agree nicely with what is reported in the experimental section.

So, at the end of step τ_2 , the structure has reached an intermediate equilibrium state where the initial surface tension related to the misfit between \bar{a} and \bar{n} is relaxed as far as possible by the drift of $\bar{\Psi}^2$. As time goes on further, \bar{n} is now allowed to relax with the characteristic time τ_n . So, during the step τ_3 , the misfit between \bar{a} and \bar{n} progressively vanishes and all variables progressively shift towards their final equilibrium values. Correlatively, $I(q)$ should reach its final value in a single exponential way within the time τ_n . Again this picture is consistent with the experimental fact that τ_3 is single exponential, q independent and ϕ^{-3} dependent.

4. Discussion.

The challenging experimental fact was the observation of the large amplitude oscillation of the scattered light intensity between two almost identical initial and final values. Our interpretation, based on the surface tension induced by the transient misfit between the surface area density and connectivity density, is actually capable of explaining this fact provided that B''/B' is very large. Moreover, it accounts at least qualitatively for the time evolution of $I(q)$.

So, we expect that i) τ_1 is the diffusion time corresponding to the collective diffusion of concentration fluctuations ; ii) τ_2 (or more precisely its single exponential tail) is τ_Ψ the relaxation time of the symmetry and iii) τ_3 is τ_n the relaxation time of the connectivity. If our interpretation is correct, the T-jump technique then appears as a very powerful technique providing detailed information on the dynamic of the sponge phase.

However, some points must be discussed at little bit further. A basic assumption of our interpretation is that the respective susceptibilities of Ψ and n have very different magnitudes ($B''/B' \gg 1$). At the present time, we do not know how to measure these two quantities independently. However, as discussed at length in [8], the static structure factor of L_3 phases at least bears two components having different q dependences : one arises from the indirect contribution (*via* the quadratic coupling) of Ψ fluctuations and the other one arising from the direct fluctuations of ϕ (membrane concentration). Static light scattering measurements performed on various systems [5, 8, 10] (among which the present one) have shown that the Ψ contribution is always appreciable. Since the coupling between Ψ and ϕ is *quadratic* (and therefore weak) this implies that, even far from critical conditions (moderate ϕ range) the susceptibility of Ψ is very much larger than that of ϕ . This observation is indeed in favour of our assumption but we cannot conclude definitely in the absence of any estimate of the susceptibility of n .

B'' actually controls, in our picture, all characteristic features of the $I(q)$ oscillation. The higher is B'' , the stronger the transient tension. Since the amplitude $\Delta I/I$ of the transient effect is related to that of the transient tension, we expect that a lower B'' will determine lower amplitudes. On the other hand, as shown in a preceding section :

$$\tau_3 = \tau_n \sim (\partial^2 f / \partial n^2)^{-1}$$

Since $\partial^2 f / \partial n^2 \sim B''$, τ_3 is again directly controlled by the actual value of B'' . Although the $L_3 \rightarrow L_\alpha$ phase transition is actually first order, we may consider that when approaching the transition temperature the structure hesitates more and more between a high connectivity density (L_3) and a very low connectivity density (L_α). We therefore expect B'' to vanish somewhere below (but close to) the transition temperature. So, the experimental observations of diverging τ_3 (Fig. 7) and vanishing A_3 (Fig. 8) are again consistent with our picture. The situation with τ_2 (Fig. 5) is not as straightforward. In order to interpret rigorously its evolution

with T , one has to work out completely the time evolution of $\langle \Psi^2(t) \rangle$ including the feedback effect on the transient tension $\gamma(t)$ (see expression (15), (16) and (18)). This is a difficult procedure which is presently beyond our capabilities. So, although the evolution of τ_2 in figure 5 seems natural in comparison with that of τ_3 , we can stress no definite statement on its consistency with our description at the present time.

There is a point however where our interpretation fails to provide a very clear explanation. This point is the level of the scattered intensity in the intermediate transient equilibrium state at the end of step τ_2 . In figure 2, this level is clearly below the initial and final levels, and this observation pertains whatever the values of ϕ , q and T . In our interpretation, $\overline{\Psi^2}$ in the intermediate state is larger than both $\overline{\Psi_{(0)}^2}$ and $\overline{\Psi_{(\infty)}^2}$ so we expect that, consistently with this enhancement of Ψ fluctuations, $I(q)$ should be above rather than below the initial and final values. Indeed, one might object that this expectation is implicitly based on the assumption of a monotonic connection between the average square amplitude of Ψ fluctuation and the measured intensity. Actually, the scattered intensity measures $\langle a_q a_{-q} \rangle$. It is nevertheless indirectly sensitive to changes in the Ψ fluctuations through the terms in H (or H_1) that couples Ψ^2 , n and a . Since these couplings are quite complicated, the postulated monotonic connexion should be questioned in more detail. Nevertheless, it seems unlikely that a more complex connexion would explain the systematic puzzling observation. Another possibility is that the ΔT steps that are sufficient to produce an appreciable $\Delta I(q)$ response, actually induce a transient excess tension large enough to trigger the symmetric/asymmetric transition. In this picture, the initial increase (τ_1) of $I(q)$ would correspond to a spinodal decomposition related to the transiently negative value of B'_1 . The lower level of $I(q)$ after τ_2 (or τ_ψ) could be explained by the well known fact [8] that the asymmetric L_3 scatters light less than the symmetric one. However, this scenario, involving the symmetry breaking at large scale, implies that some well defined threshold exists for the ΔT step beyond which the transition is triggered. The experimental observation (Fig. 3) rather indicates a quite linear variation the $I(q)$ oscillation. In order to investigate this point in more detail, we performed some measurements under very low ΔT steps (less than 0.1 °C). It seems that a threshold actually exists but the signal to noise ratio of the response under such a low excitation is not good enough for any definite statement. Clearly, more experimental work is to be done in order to clarify the puzzling point reported in this last paragraph. We are presently in the course of improving the design of the experimental set up and we hope that we shall soon be able to investigate the very low ΔT range.

References

- [1] PORTE G., MARIGNAN J., BASSEREAU P., MAY R., *J. Phys. France* **49** (1988) 511.
- [2] GAZEAU D., BELLOCQ A., ROUX D., *Europhys. Lett.* **9** (1989) 447.
- [3] STREY R., SCHOMACKER R., ROUX D., NALLET F., OLSSON U., *J. Chem. Soc. Faraday Trans.* **86** (1990) 2253.
- [4] PORTE G., APPELL J., BASSEREAU P., MARIGNAN J., *J. Phys. France* **50** (1989) 447.
- [5] PORTE G., DELSANTI M., BILLARD I., SKOURI M., APPELL J., MARIGNAN J., DEBEAUVAIS F., *J. Phys. II France* **1** (1991) 1101.
- [6] SNABRE P., PORTE G., *Europhys. Lett.* **13** (1990) 641.
- [7] MILNER S. T., CATES M. E., ROUX D., *J. Phys. France* **51** (1990) 2629.
- [8] ROUX D., CATES M. E., OLSSON U., BALL R. C., NALLET F., BELLOCQ A. M., *Europhys. Lett.* **11** (1990) 229.
- [9] CANDAU S., MERIKKI F., WATON G., LEMARÉCHAL P., *J. Phys. France* **51** (1990) 977.
- [10] COULON C., ROUX D., BELLOCQ A. M., *Phys. Rev. Lett.* **66** (1991) 1709.
- [11] DAVID F., LEIBLER S., *J. Phys. II France* **1** (1991) 959.